Solid and Liquid Metastable Phase Equilibria in the Aqueous Quaternary System Li^+, Mg^{2+}//SO_4^{2-}, Borate-H_2O at 273.15 K

MENG Lingzong[1,2,3*], GUO Yafei[1,2], LI Dan[2,3] and DENG Tianlong[1*]

1. Tianjin Key Laboratory of Marine Resources and Chemistry, College of Chemical Engineering and Material Sciences, Tianjin University of Science and Technology, Tianjin 300457, P. R. China;

2. School of Chemistry and Chemical Engineering, Linyi University, Linyi 276005, P. R. China;

3. CAS Key Laboratory of Salt Lake Resources and Chemistry, Qinghai Institute of Salt Lakes, Chinese Academy of Sciences, Xining 810008, P. R. China

Abstract The metastable phase equilibria of the Li^+, Mg^{2+}//SO_4^{2-}, borate-H_2O system at 273.15 K were studied using isothermal evaporation method. The dry-salt phase diagram, water-phase diagram and the physicochemical property diagrams of the system were plotted with the metastable solubility values and physicochemical properties corresponding to density, refractive index, pH value and conductivity. The dry-salt diagram was composed of four crystallizing zones[lithium sulfate hydrate($Li_2SO_4·H_2O$), epsomite($MgSO_4·7H_2O$), lithium metaborate octahydrate($LiBO_2·8H_2O$), and hungchaoite($MgB_4O_7·9H_2O$)], five univariant curves and two invariant points ($Li_2SO_4·H_2O$+$MgSO_4·7H_2O$+$MgB_4O_7·9H_2O$ and $Li_2SO_4·H_2O$+$LiBO_2·8H_2O$+$MgB_4O_7·9H_2O$). $Li_2B_4O_7$ converted into $LiBO_2$ in solution. Comparing the metastable phase diagram at 273.15 K and stable phase diagram at 298.15 K for the system, the crystallized area of $Li_2SO_4·H_2O$ and $MgSO_4·7H_2O$ became large, whereas, the other phase regions became small. The $J(H_2O)$ changes regularly with increasing $J(SO_4^{2-})$, and the physicochemical properties change regularly with the concentration of $B_4O_7^{2-}$ increasing.

Keywords Metastable phase equilibrium; Phase diagram; Solubility; Lithium metaborate octahydrate; Hungchaoite

1 Introduction

Lithium and boron are very important elements used in industry and technology fields. The salt-lake brines in Qinghai-Tibet plateau have high lithium and boron contents[1]. The brine is considered as a complex five-component system of Li^+, Mg^{2+}//Cl^-, SO_4^{2-}, borate-H_2O after the minerals of NaCl and KCl are crystallized and separated[2]. It is well known that phase equilibria and phase diagrams are both theoretical foundations for exploiting the brine and describing the geochemical behavior of brine and mineral systems[3—5]. The solar pond technique is widely used in the exploitation of brine resources. The crystal formation of evaporated brines usually follows the metastable phase diagram[6]. Therefore, the metastable phase equilibria of the brine system are necessary to exploit the lithium and boron in the brine.

The stable and metastable phase equilibrium for many systems containing lithium, magnesium, chloride, sulfate and borate have been reported in the literature[7—9]. The Li^+, Mg^{2+}//SO_4^{2-}, $B_4O_7^{2-}$-H_2O system is an important subsystem of the above-mentioned quaternary system. The stable phase diagram of the quaternary system at 298.15 K has been studied previously[10]. $MgB_4O_7·9H_2O$ and $Li_2B_4O_7·3H_2O$ formed in the system at 298.15 K. $MgB_4O_7·9H_2O$ has the largest crystallization area in the system because it is the least soluble. Considering the average temperature of the brine during Qinghai-Tibet plateau winter is about 273.15 K, the metastable phenomenon for borate is notable. Therefore, the metastable phase equilibrium at 273.15 K has significant value for boron exploitation. In this study, the solubility and physicochemical properties of the quaternary system Li^+, Mg^{2+}//SO_4^{2-}, borate-H_2O at 273.15 K were determined.

2 Experimental

2.1 Reagents and Apparatus

$Li_2SO_4·H_2O$(Shanghai Guoyao Chemical Reagent Corp., initial mass purification fraction: 99.0%, final mass fraction after recrystallization: 99.5%); $MgSO_4·7H_2O$(Tianjin Kermel Chemical Reagent Ltd., initial mass fraction 99.0%, final mass fraction after recrystallization: 99.5%); $Li_2B_4O_7$(Tianjin Kermel

*Corresponding authors. E-mail: menglingzong@lyu.edu.cn; tldeng@tust.edu.cn

Received October 8, 2016; accepted November 21, 2016.

Supported by the National Natural Science Foundation of China(Nos.21406104, U1407113, U1507112 and U1607123), the China Postdoctoral Science Foundation(No.2015M581303), the Yangtze Scholar and Innovative Research Team in Chinese University(No.IRT_17R81) and the Fund of Key Laboratory of Salt Lake Resources and Chemistry, Qinghai Institute of Salt Lake, Chinese Academy of Sciences in China (No.KLSLRC-KF-13-HX-2).

Chemical Reagent Ltd., mass fraction 99.0%); Hungchaoite ($MgB_4O_7·9H_2O$ synthesized in our laboratory with the method in the literature[11], mass fraction 99.0%). Doubly deionized water(conductivity less than $1.2×10^{-4}$ S/m, pH 6.60 at 298.15 K) was used for the experimental solutions and chemical analysis. The isothermal evaporation apparatus was installed for the experiments, which is described detailedly in our previous work[8]. An XP-300 Digital Polarizing Microscopy(Shanghai Caikon Optical Instrument Co., Ltd., China) and an X-ray diffractometer(X'pert PRO, Spectris. Pte. Ltd., the Netherlands) were employed for the identification of the solid phases.

2.2 Experimental Method

Isothermal evaporation was used to determine the metastable phase equilibrium[8]. In clean polyethylene containers(isothermal evaporation containers), the solution temperature was maintained at 273.15 K(uncertainty less than 0.1 K) during the evaporation process. Clarified solutions were transferred for chemical analysis if new solid mineral crystals formed. The solution concentration was equal to the metastable solubility. For one evaporated container of solution, numerous solubility data could be obtained. Solubility curves were drawn in the phase diagrams by connecting enough solubility points with the same solid phases.

Polarizing microscopy with oil immersion was employed for solid phase identification. Take the mixed minerals of $LiBO_2·8H_2O$ and $MgB_4O_7·9H_2O$ for example, as for the minerals of $LiBO_2·8H_2O$ and $MgB_4O_7·9H_2O$, the former belongs to a hexagonal system and monoaxial, optically negative crystal, *i.e.*, (–), whereas, the later belongs to a monoclinic system and dual, optically positive crystal, *i.e.*, 2*v*(–). And the minerals $LiBO_2·8H_2O$ and $MgB_4O_7·9H_2O$ can also be identified through the refractive index measurement.

2.3 Analytical Method

The sulfate ion concentration(SO_4^{2-}) in the solutions was measured with the gravimetric method using barium chloride(uncertainty of ±0.0005). The boron ion concentration($B_4O_7^{2-}$) was analysed by titration in the presence of mannitol with NaOH solution(precisions within ±0.003)[12]. The magnesium ion(Mg^{2+}) concentration was analysed with the modified edathamil disodium(EDTA) complexometric titration method in the presence of Eriochrome Black-T as indicator(precisions within ±0.003)[13]. The lithium ion(Li^+) concentration was calculated with the charge balance and validated with ICP-AES method(precisions within ±0.005). The physicochemical property measurement methods were the same as those in the literature[8]. The difference for this work is that the temperature for physicochemical property analysis is (273.15±0.1) K.

3 Results and Discussion

The metastable experimental solubility of the Li^+, $Mg^{2+}//SO_4^{2-}$, borate-H_2O system at 273.15 K was measured, and the results are presented in Table 1. Using the Jänecke index[*J*/(mol/100 mol dry salt)], the metastable dry-salt

Table 1 Solubilities of the Li^+, $Mg^{2+}//SO_4^{2-}$, borate-H_2O system at 273.15 K

No.	*w*(%)				Jänecke index, *J*/(mol/100 mol dry salt)			Equilibrium solid phase*
	Li^+	Mg^{2+}	SO_4^{2-}	$B_4O_7^{2-}$	$J(SO_4^{2-})$	$J(2Li^+)$	$J(H_2O)$	
1(E_1)	2.65	2.07	26.52	0.00	100	69.21	1377.40	Ls + Eps
2	2.60	2.26	26.61	0.51	98.83	66.79	1347.23	Ls + Eps
3	2.50	2.28	25.91	0.71	98.33	65.75	1388.22	Ls + Eps
4	2.54	2.41	26.30	1.28	97.07	64.79	1327.76	Ls + Eps
5	2.50	2.40	2.60	1.30	96.99	64.62	1347.35	Ls + Eps
6	2.45	2.50	25.71	1.81	95.83	63.23	1341.97	Ls + Eps
7	2.36	2.78	23.78	5.69	87.10	59.82	1277.09	Ls + Eps
8(E)	2.34	2.89	23.63	6.50	85.40	58.66	1244.88	Ls + Eps + Mb
9(E_2)	0.00	4.33	15.51	2.94	89.50	0.00	2374.11	Eps + Mb
10	0.45	3.81	16.29	3.08	89.52	17.16	2236.97	Eps + Mb
11	1.45	3.50	21.88	3.19	91.72	42.09	1564.54	Eps + Mb
12	1.73	3.12	22.31	3.21	91.82	49.23	1528.17	Eps + Mb
13	2.00	3.04	23.10	4.49	89.27	53.59	1388.05	Eps + Mb
14(E_3)	3.60	0.00	22.58	3.73	90.71	100	1502.07	Ls + Lb
15	3.57	0.07	21.57	5.56	86.25	98.92	1476.17	Ls + Lb
16	3.46	0.34	21.04	6.86	83.22	94.61	1440.88	Ls + Lb
17(F)	3.62	0.59	22.56	7.73	82.50	91.50	1277.16	Ls + Lb + Mb
18(E_4)	0.31	0.02	0.00	3.54	0.00	97.00	23371.8	Lb + Mb
19	1.24	0.09	2.26	10.76	25.32	95.93	5122.76	Lb + Mb
20	3.34	0.26	13.13	17.87	54.29	95.67	1441.82	Lb + Mb
21	3.73	0.27	15.38	18.53	57.29	96.06	1233.17	Lb + Mb
22	3.90	0.20	17.82	16.07	64.18	97.12	1190.55	Lb + Mb
23	3.62	0.31	17.43	14.24	66.41	95.40	1308.94	Lb + Mb
24	3.50	0.35	19.94	9.13	77.92	94.60	1397.77	Lb + Mb
25	3.50	0.77	24.07	5.14	88.32	88.78	1301.48	Ls + Mb
26	2.91	1.17	23.62	1.81	95.46	81.37	1519.30	Ls + Mb
27	2.75	1.66	24.03	2.55	93.84	74.34	1436.97	Ls + Mb
28	2.55	2.55	24.70	4.93	89.01	63.62	1254.12	Ls + Mb

* Ls: $Li_2SO_4·H_2O$; Eps: $MgSO_4·7H_2O$; Lb: $LiBO_2·8H_2O$; Mb: $MgB_4O_7·9H_2O$.

diagram of the system at 273.15 K is presented in Fig.1. The phase diagram in Fig.1 is composed of four crystallizing zones[lithium sulfate hydrate($Li_2SO_4·H_2O$, Ls), epsomite($MgSO_4·7H_2O$, Eps), lithium metaborate octahydrate($LiBO_2·8H_2O$, Lb), and hungchaoite($MgB_4O_7·9H_2O$, Mb)], five univariant solubility curves co-saturated with two salts[E_1E(Ls+Ms), E_2E(Eps+Mb), EF(Ls+Mb), E_3F(Ls+Lb) and E_4F(Lb+Mb)], and two invariant points co-saturated with three salts [E(Ls+Eps+Mb) and F(Ls+Lb+Mb)]. The crystallization area of $MgB_4O_7·9H_2O$, shown in Fig.1, is the largest of the four zones because it is the least soluble. There are neither solid solutions nor double salts crystallized from the solutions. The X-ray diffraction patterns for solid phases in the invariant points are given in Fig.2. The single and orthogonal polarized light crystal images generated from polarized microscopy with oil immersion on representative solid phases for the invariant points E are presented in Fig.3. Fig.2 and Fig.3 show that the coexisting solid phase equilibria at invariant points E and F were(Ls+Eps+Mb) and (Ls+Lb+Mb), respectively.

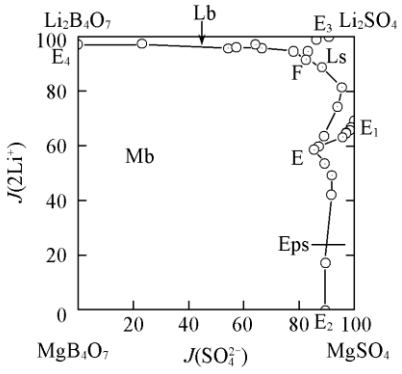

Fig.1 Dry-salt phase diagram of the Li^+, Mg^{2+}//SO_4^{2-}, borate-H_2O system at 273.15 K

○ Solubility data in this work; —, experimental stable isotherm curve; Ls: $Li_2SO_4·H_2O$; Eps: $MgSO_4·7H_2O$; Lb: $LiBO_2·8H_2O$; Mb: $MgB_4O_7·9H_2O$.

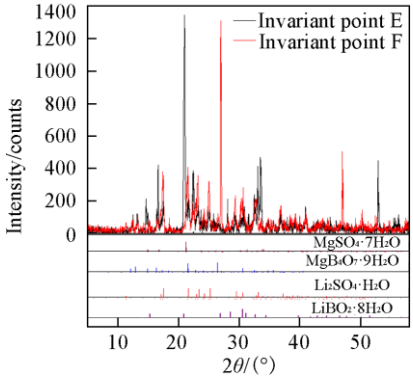

Fig.2 XRD patterns of the coexisted solid phases in the invariant points

Although $Li_2B_4O_7$ was added with other salts and loaded into clean polyethylene containers at the beginning, $LiBO_2·8H_2O$ rather than $Li_2B_4O_7·3H_2O$ was found to crystallize from the solution through a series of mineral identifications. $Li_2B_4O_7$ in the solution converted into $LiBO_2$. Boron ion in the solution was no longer in the form of $B_4O_7^{2-}$, but $B_4O_7^{2-}$ was still used to express the concentration of borate and calculate the Jänecke index of borate for convenience in this work.

Due to the lack of solubility data for the stable equilibrium

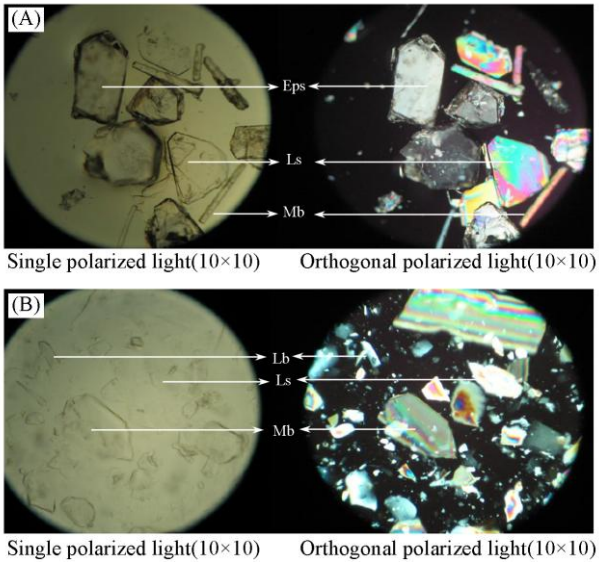

Fig.3 Identification of the invariant for the solid phase in the reciprocal system with polarized microscopy using an oil immersion method

(A) Invariant point E; (B) invariant point F; Ls: $Li_2SO_4·H_2O$; Eps: $MgSO_4·7H_2O$; Lb: $LiBO_2·8H_2O$; Mb: $MgB_4O_7·9H_2O$.

system at 273.15 K in the literature, a comparison between the metastable phase diagram at 273.15 K(solid line) and the stable phase diagram at 298.15 K[10](dashed line) is shown in Fig.4. The crystallizing zone of $Li_2B_4O_7·3H_2O$ in the stable equilibrium converted into $LiBO_2·8H_2O$ in the metastable equilibrium. The stable maximum concentration for $B_4O_7^{2-}$ at 298.15 K was approximately 2.71%[6], but in the metastable equilibrium at 273.15 K, the maximum concentration for $B_4O_7^{2-}$ was 18.53%. This suggests that the metastable phenomenon of the borate solution was clearly observed in the isothermal evaporation process. Compared to stable solubility values at 298.15 K, the metastable solubility for $Li_2SO_4·H_2O$ and $MgSO_4·7H_2O$ decreased at 273.15 K, but the metastable solubility for borate significantly increased at 273.15 K. Therefore, the crystallized areas of both $Li_2SO_4·H_2O$ and $MgSO_4·7H_2O$ were enlarged; whereas, the borate metastable phase regions decreased significantly, as shown in Fig.4. The variation in solubility was

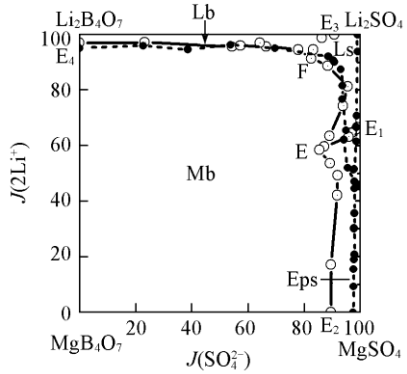

Fig.4 Comparison of the metastable dry-salt-phase diagram at 273.15 K and stable dry-salt phase diagram at 298.15 K in the Li^+, Mg^{2+}//SO_4^{2-}, borate-H_2O system

○ Metastable data; — metastable curve; ● stable data; ⋯ stable curve; Ls: $Li_2SO_4·H_2O$; Eps: $MgSO_4·7H_2O$; Lb: $LiBO_2·8H_2O$; Mb: $MgB_4O_7·9H_2O$.

caused by temperature and the different state between stable and metastable equilibrium. This solubility information can be applied for lithium and boron exploiting.

The water-phase diagram, drawn with the $J(H_2O)$ data in Table 1, is presented in Fig.5. The $J(H_2O)$ changes regularly with increasing $J(SO_4^{2-})$. The largest and smallest $J(H_2O)$ values were at points E_4 and E, which illustrates the solubility values of borate were smaller than other salts in this system. The water-phase diagram was used to calculate water loss in the evaporation process for the brine, which is a key factor for exploiting brine resources.

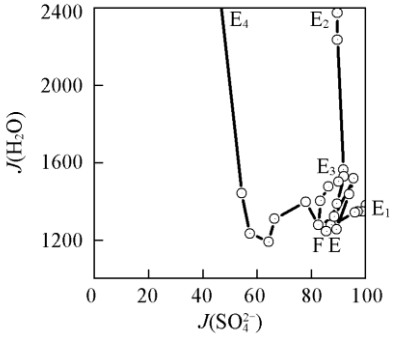

Fig.5 Water-phase diagram of the Li^+, Mg^{2+}//SO_4^{2-}, borate-H_2O system at 273.15 K

○ Solubility data in this work; — experimental water-phase isotherm curve.

The physicochemical property diagrams(density, refractive index, pH value and conductivity), presented in Fig.6, were obtained using the data in Table 2. The abscissa data were composition of $B_4O_7^{2-}$(in mass fraction), which were different from that in Fig.5. The physicochemical property curves are complex and change regularly with $B_4O_7^{2-}$ concentration. The curves in the density diagram and refractive index diagram were nearly the same, with maximum values at point E and minimum values at point E_4. The conductivity curves also showed minimum values at point E_4, but the pH curves gave maximum values at point E_4. The solution of the system was alkaline because of the boron ions, and the pH was between 7.20 and 9.32. Therefore, the invariant points co-saturated with two or three salts were evaluated from the physicochemical property data.

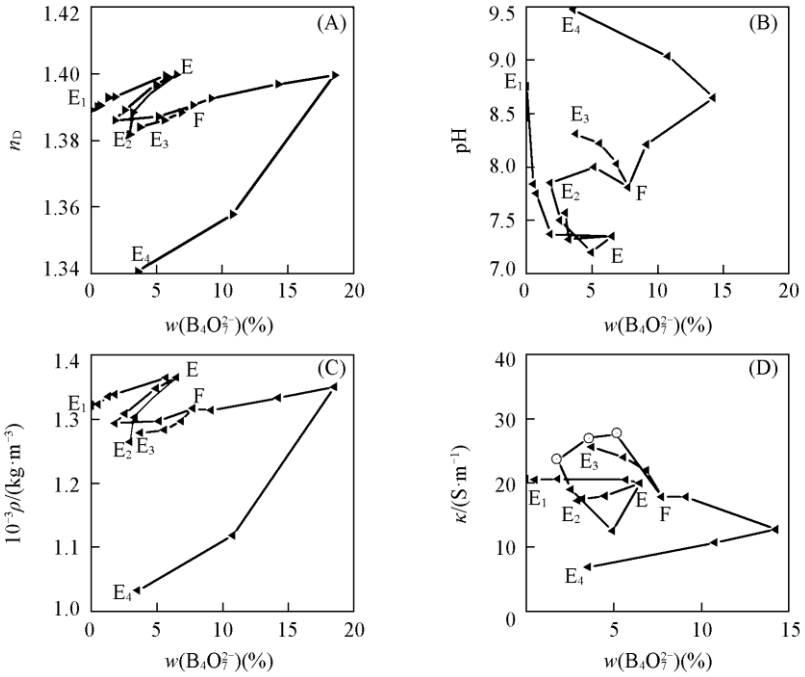

Fig.6 Physicochemical properties *vs.* composition diagrams of the Li^+, Mg^{2+}//SO_4^{2-}, borate-H_2O system at 273.15 K

Table 2 Physicochemical properties of the Li^+, Mg^{2+}//SO_4^{2-}, borate-H_2O system at 273.15 K*

No.	n_D	pH	$10^{-3}\rho$/(kg·m^{-3})	κ/(S·m^{-1})	No.	n_D	pH	$10^{-3}\rho$/(kg·m^{-3})	κ/(S·m^{-1})
1(E_1)	1.3892	8.76	1.3219	20.60	15	1.3861	8.22	1.2832	—
2	1.3901	7.84	1.3233	23.50	16	1.3884	8.03	1.2968	21.00
3	1.3905	7.75	1.3233	19.23	17(F)	1.3906	7.81	1.3168	17.84
4	1.3930	7.32	1.3355	35.70d	18(E_4)	1.3407	9.48	1.0322	6.94
5	1.3928	—	—	—	19	1.3578	9.04	1.1185	15.71
6	1.3931	7.37	1.3387	16.63	20	—	—	—	—
7	1.3995	—	1.3644	—	21	1.3996	—	1.3504	—
8(E)	1.3998	7.35	1.3652	—	22	—	—	—	—
9(E_2)	1.3818	7.57	1.2644	19.25	23	1.3969	8.65	1.3334	12.78
10	—	—	—	—	24	1.3926	8.21	1.3139	17.84
11	1.3910	8.01	1.3176	17.09	25	1.3832	8.00	1.2771	27.50
12	1.3916	7.32	1.3198	17.52	26	1.3861	7.85	1.2932	23.60
13	—	—	—	—	27	1.3891	7.50	1.3086	—
14(E_3)	1.3840	8.31	1.2788	25.60	28	1.3978	7.20	1.3583	12.57

* — Not detected.

4 Conclusions

The metastable solubility data and physicochemical property data of the Li^+, Mg^{2+}//SO_4^{2-}, borate-H_2O system at 273.15 K were studied using isothermal evaporation method. The dry-salt diagram was composed of four crystallizing regions($Li_2SO_4·H_2O$, $MgSO_4·7H_2O$, $LiBO_2·8H_2O$, and $MgB_4O_7·9H_2O$), two invariant points co-saturated with three salts, and five univariant curves co-saturated with two salts. When comparing the stable diagram at 298.15 K and the metastable diagram at 273.15 K, the crystallized regions of $Li_2SO_4·H_2O$ and $MgSO_4·7H_2O$ became larger, while those of $LiBO_2·8H_2O$, and $MgB_4O_7·9H_2O$ became smaller in the metastable diagram. The $J(H_2O)$ changed regularly with increasing $J(SO_4^{2-})$, and the physicochemical properties changed regularly with the concentration of $B_4O_7^{2-}$ increasing in the solution.

References

[1] Zheng X. Y., Tang Y., Xu C., *Tibet Saline Lake*, Chinese Science Press, Beijing, **1988**

[2] Sun B., Song P. S., Du X. H., *J. Salt Lake Res*., **1994**, *2*(4), 26

[3] Li Z. W., Qian Z. P., Chen X., Dang Y. L., Yang Q. C., *Chem. J. Chinese Universities*, **2015**, *36*(9), 1759

[4] Huang Y., Zou F., Ni S. J., Sang S. H., *Chem. Res. Chinese Universities*, **2011**, *27*(3), 482

[5] Li L., Zhang S. S., Liu Y. H., Guo Y. F., Deng T. L., *Chem. J. Chinese Universities*, **2016**, *37*(2), 349

[6] Song P. S., Sun B., Zeng D. W., *Pure Appl. Chem.*, **2013**, *85*(11), 2097

[7] Meng L.Z., Li D., *Braz. J. Chem. Eng.*, **2014**, *31*(1), 251

[8] Deng T. L., Meng L. Z., Sun B., *J. Chem. Eng. Data*, **2008**, *53*(3), 704

[9] Gao D. L., Guo Y. F., Yu X. P., Wang S. Q., Deng T. L., *J. Chem. Eng. Data*, **2015**, *60*(9), 2594

[10] Song P. S., Fu H. A., *J. Inorg. Chem*., **1991**, *7*(3), 344

[11] Jing Y., *Sea-lake Salt and Chemical Industry*, **2000**, *29*(2), 24

[12] Zhai Z. X., *Analytical Methods of Brines and Salts*, 2nd Ed., Chinese Science Press, Beijing, **1988**

[13] Wang S. Q., Gao J., Yu X., Sun B., Deng T. L., *J. Salt Lake Res*., **2007**, *15*, 44